

Enhanced collision induced desorption and dissociation of O₂ chemisorbed on Ag(001) at grazing incidence

L. Vattuone¹, P. Gambardella, F. Cemič, U. Valbusa, M. Rocca

INFN and Centro di Fisica delle Superfici e delle Basse Temperature del C.N.R., Dipartimento di Fisica, via Dodecaneso 33, 16146 Genova, Italy

Received 21 February 1997; in final form 2 September 1997

Abstract

We have investigated desorption and dissociation of O₂ chemisorbed on Ag(001) induced by collision with hyperthermal Xe and Ar atoms provided by a supersonic molecular beam. We find that the cross section for both processes increases rapidly with impact energy and with angle of incidence of the inert gas atom. A model is presented which accounts for the observed energy threshold and for the trend in the cross section. © 1997 Elsevier Science B.V.

Collision induced dissociation and desorption phenomena are suspected to play an important role in catalytic reactions run industrially at high pressure and temperature and in presence of carrier gases, by opening up new so far unexplored, pathways [1–3]. The understanding of the energetic and angular dependence of the cross section of these phenomena is at present limited to the simplest cases of physisorption [4–7]. For chemisorption [8,9] even a qualitative understanding of the energetic and angular dependence of the cross section becomes a major task as the phenomena are influenced by surface corrugation, adsorption geometry and energy transfer to the surface. This problem is considered in this Letter with new measurements of the angular and of the energetic dependence of the cross section for desorption and dissociation of chemisorbed dioxygen on Ag(001) induced by Xe bombardment, in conjunc-

tion with molecular dynamics simulations. The occurrence of collision induced dissociation and desorption for O₂ chemisorbed on Ag(110) has been recently demonstrated [10] but the dependence of the cross section on the angle of incidence was not investigated. We shall show that the cross section for both phenomena increases rapidly with the energy and angle of incidence of the hyperthermal Xe atom. While the former effect is expected and indicates that the process is activated, the latter is new and of surprising magnitude (a factor 40 when varying the angle, θ_i from 0° to 60°). Interestingly this has not been observed for any chemisorbed system investigated so far. Employing a simple model we find that the effect is due to the corrugation of the interaction potential and to the softness (low Debye temperature) of the Ag surface, which causes substantial energy transfer to phonons.

The experiment was performed with the apparatus described in Ref. [11]. The sample, an Ag(001) single crystal, is cleaned in UHV by Ar or Ne ion sputtering and annealing cycles; the cleanliness is

¹ Corresponding author.

checked by high resolution electron energy loss spectroscopy (HREELS). Firstly molecular oxygen is dosed on the sample kept at liquid nitrogen temperature, using a supersonic molecular beam. Exposure to the Xe beam follows. After dosing with O₂ and after each exposure to Xe, a HREEL- spectrum is recorded. Both the oxygen and Xe are seeded in He so that translational energies as high as 0.8 eV for O₂ and 2.7 eV for Xe can be obtained. Fig. 1 shows the EEL spectra recorded in a typical experimental run.

Oxygen was predosed at a given exposure (18 s exposure to O₂ at an energy $E_{O_2} = 0.39$ eV corresponding to a coverage $\Theta_{O_2} = 0.19$ ML, as calibrated by thermal desorption (TDS) [12–14]) chosen so that the corresponding coverage is at the upper limit for which the normalized integrated intensity of the losses around 80 meV (corresponding to the intramolecular stretching motion of the chemisorbed O₂ molecules [15]) is approximately linear in the molecular oxygen coverage Θ_{O_2} [13]. The EEL intensity

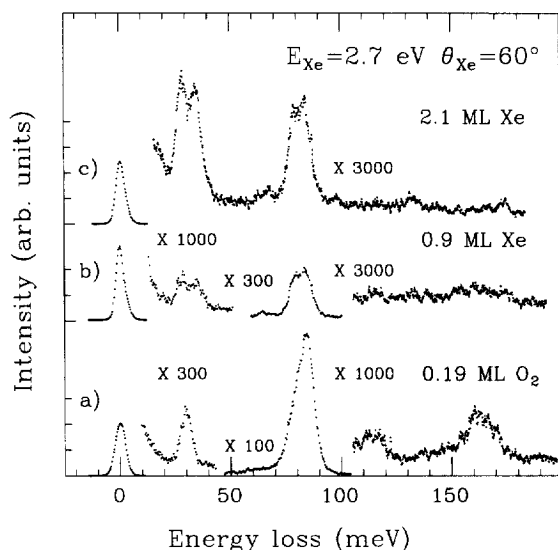


Fig. 1. EEL spectra for Xe atoms of energy $E_{Xe} = 2.7$ eV impinging on the surface at an angle $\theta_{Xe} = 60^\circ$ from the normal, recorded in-specular with electron energy $E_e = 3.3$ eV at an angle $\theta_e = 63^\circ$ from the surface normal. The spectrum (a) was recorded after 18 s exposure to a beam of oxygen (3%) seeded in He (97%) with the nozzle at room temperature, corresponding to a coverage $\Theta_{O_2} = 0.19$ ML. Spectrum (b) was recorded after an exposure of 0.9 ML of Xe and spectrum (c) after 2.1 ML of Xe. The Xe flux Φ is 0.07 ML/s. 1 ML corresponds to 1.2×10^{15} atoms/(cm²), the surface density of Ag atom on Ag(001).

can thus be taken as a measure of the dioxygen coverage. The other losses associated with the O₂ ad molecules are due to the molecule-surface vibration (at 30 meV), with a combination band (at 114 meV) and with an overtone (at 164 meV) [13]. In contrast to the losses at 80 meV, the loss at 30 meV does not exhibit a linear behaviour in the same coverage range [13] and thus cannot be taken as a measure of Θ_{O_2} . The loss at 35 meV is due to atomic oxygen and is proportional to the atomic oxygen coverage Θ_O . As one can see that as soon as the system is exposed to the hyperthermal Xe beam, the intensities of the losses at 30 and at 80 meV decrease, the latter showing its reported doublet nature [16]. In contrast the loss at 35 meV (dissociated oxygen), initially absent, shows up and increases. The molecular oxygen intensity is calibrated from the initial O₂ coverage while for the O-Ag(001) mode we have assumed the dipole moment to be the same as for O-Ag(110). This introduces a systematic uncertainty in the atomic oxygen coverage of not larger than 50% which does not however affect our conclusions. Θ_{O_2} and Θ_O are shown in Fig. 2 as a function of exposure to Xe for two measurements taken at the same total energy $E_{Xe} = 2.7$ eV but at different impact angles $\theta_{Xe} = 0^\circ$ and $\theta_{Xe} = 60^\circ$.

It is apparent that most O₂ molecules desorb due to collisions with hyperthermal Xe while a smaller fraction dissociates. It is also evident that the decrease in the O₂ coverage with exposure to Xe is much faster at grazing than at normal incidence. Note the factor 100 in magnitude difference in the exposure scale. The effect is monotonic with θ in contrast with the findings of Szulcowski et al. [8] for NH₃ on Pt(111) and of Ceyer for CO on Ni(111) [4]. The detailed analysis of the different behaviour of the two O₂ moieties will be reported elsewhere [17]. The balance equations for molecular and atomic oxygen read:

$$\frac{d\Theta_{O_2}}{dt} = -(\Sigma_{des} + \Sigma_{diss})\Phi\Theta_{O_2}, \quad (1)$$

$$\frac{d\Theta_O}{dt} = 2\Sigma_{diss}\Phi\Theta_{O_2}, \quad (2)$$

where Φ is the xenon flux (0.07 ML/s, as measured by a spinning rotor gauge) and Σ_{des} and Σ_{diss} are the

cross sections for desorption and dissociation, respectively. Assuming that the total cross section, $\Sigma_{\text{des}} + \Sigma_{\text{diss}}$, is linear in Θ_{O_2} , we can solve the differential equations and determine Σ_{des} and Σ_{diss} by fitting the data of Fig. 2. The initial cross sections for desorption and dissociation (at 0.19 ML) are shown in Fig. 3 as a function of energy E and impact angle θ . The values of the best fit parameters and their errors are evaluated by a standard Minuit routine, assuming the error on the molecular and atomic oxygen coverages to be 0.01 ML.

As one can see, Σ_{des} and Σ_{diss} increase with E for both Ar and Xe. The comparison between Xe and Ar data is possibly complicated by the different mass ratio with O_2 and Ag which affects the energy transfer in the collision process. We will deal with this problem elsewhere [17]. In this Letter we would like to focus on the unexpected result that both Σ_{des} and Σ_{diss} are greater than one order of magnitude smaller at normal than at grazing incidence.

To our knowledge such an enhancement at grazing incidence has not been observed for any previous systems, some of which exhibited an increase smaller than a factor 2 in Σ_{des} with θ (as for Ar-CH_4 –

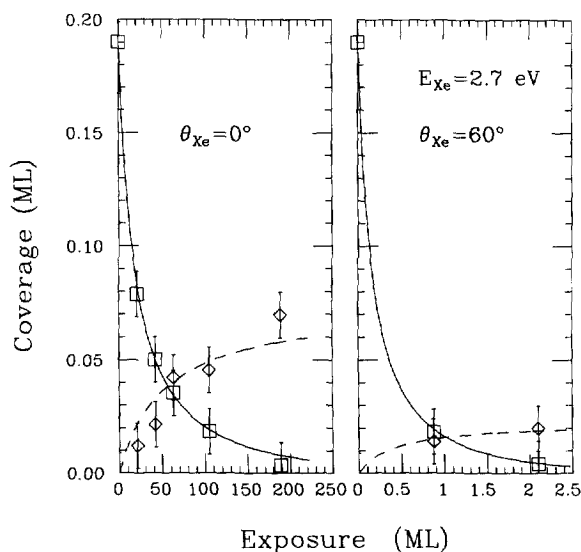


Fig. 2. The total O_2 coverage (\square) and the atomic oxygen coverage Θ_{O} (\diamond) as a function of exposure to xenon, for the data of Fig. 1 (right), and for the same xenon energy but at normal incidence (left). The continuous and dashed lines are the best fit obtained using the solutions to Eqs. (1) and (2).

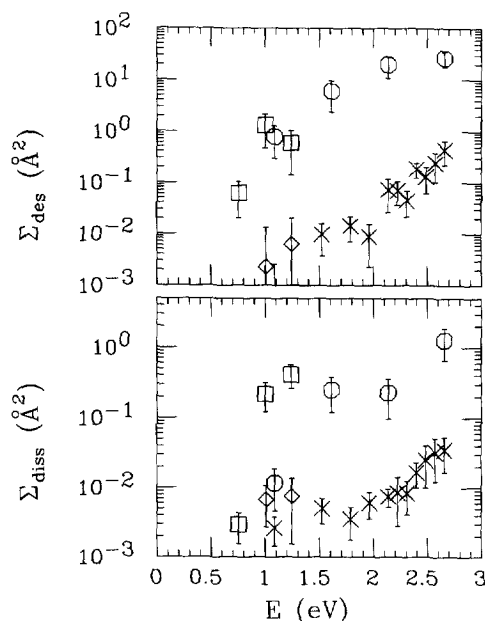


Fig. 3. Σ_{diss} (lower panel) and Σ_{des} (upper panel) as a function of Xe (or Ar) energy at 0.19 ML coverage of O_2 for $\theta = 60^\circ$, \circ (or \square); $\theta = 0^\circ$, \times (or \diamond).

Ni(111) [5]) and a comparable or even smaller increase in Σ_{diss} (as for Ar-NH_3 – Pt(111) [8] or Xe-CO-Ni(111) [4]).

The large increase in Σ_{des} and in Σ_{diss} with θ cannot be explained by geometric arguments, as it was the case for the doubling of Σ_{des} for Ar-CH_4 – Ni(111) . Mirror collisions cannot account for an increase of Σ_{des} with θ larger than a factor two; moreover they are expected to play a minor role at the relatively small molecule–surface distance of a chemisorbed system. The angular enhancement is similar for Ar and Xe, so that it cannot be ascribed to some peculiarity of the impinging atom.

In order to clarify the mechanism which causes such an increase of Σ_{des} with θ we have performed a molecular dynamic simulation, using a simple model similar to the one employed by Beckerle et al. [5]. Dissociation is not included as a more realistic and complicated description would be required; such an assumption is justified in our case by the much smaller value of Σ_{diss} with respect to Σ_{des} . The silver surface is modelled by a square array of rigid spheres with a given effective mass m_{eff} . The radius

of the Ag atom is taken as half of the Ag–Ag distance, i.e. 1.44 Å. The oxygen molecule is represented by a rigid sphere of radius 1.125 Å, intermediate between the O–O distance (1.5 Å) and the O covalent radius (0.75 Å). The Xe radius is set at its covalent value of 2.2 Å. The Ag atomic positions are fixed at the lattice site. This choice of the parameters models a (100) surface with corrugation $c_{\text{Ag}} = 1.44$ Å with O₂ chemisorbed in the fourfold hollow site. The energy transfer in the collision between the adsorbate and the substrate depends on the ratio of the mass of the adsorbate and of the effective mass of the substrate. The latter implicitly takes into account the coupling between the atoms of the substrate: the stronger such a coupling, the larger m_{eff} and the lower the possible energy transfer to the substrate. The equations of motion are analytically determined applying: (a) energy and momentum conservation and assuming a hard sphere interaction potential for the Xe–O₂ collision; (b) conservation of momentum in the direction parallel to the local surface normal and normal energy transfer E_n

$$E_n \propto 4 \frac{m m_{\text{eff}}}{(m_{\text{eff}} + m)^2}, \quad (3)$$

where m is the Xe or O₂ mass for the Xe–Ag and O₂–Ag collisions.

The initial position of the Xe atoms is randomly chosen over a square of 20×20 Å at a distance of 100 Å from the surface. The oxygen molecule is placed at the fourfold hollow site at a chemisorption distance of 0.43 Å from the geometrical surface plane. The O₂ molecule was assumed to have desorbed if (a) its normal kinetic energy is larger than the binding energy and (b) its velocity is directed away from the surface.

The results were obtained by running 10^4 trajectories for each energy and angle. The relative error on Σ_{des} is then proportional to $1/\sqrt{N_{\text{des}}}$, where N_{des} is the number of trajectories ending with desorption of O₂. Fig. 4 shows the cross section for desorption as a function of E_{Xe} at normal and grazing incidence (60°) for two values of the effective mass m_{eff} of the Ag atoms on a strongly corrugated surface. The result in the upper panel ($m_{\text{eff}} = 1500$ amu) corresponds to the limit of a hard material where several atoms of the substrate are involved in the collision

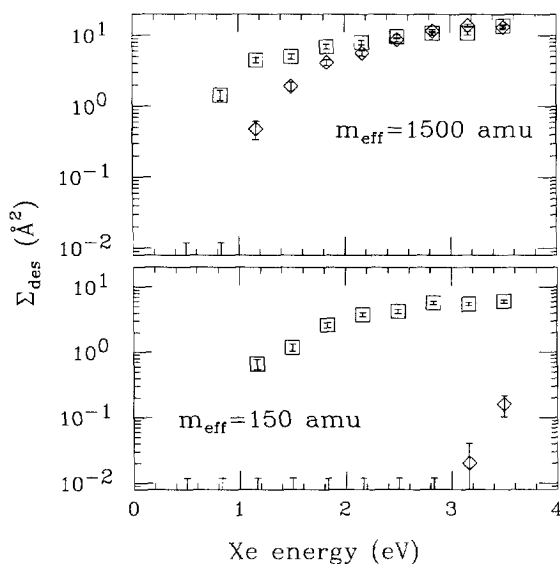


Fig. 4. Calculated cross section for desorption on a corrugated surface ($c_{\text{Ag}} = 1.44$ Å), for different values of m_{eff} . \diamond : $\theta_{\text{Xe}} = 0^\circ$; \square : $\theta_{\text{Xe}} = 60^\circ$.

and only a small energy loss to the substrate takes place. In the lower panel, however, m_{eff} is equal to 150 amu, i.e. approximately 1.5 times the mass of the free Ag atom and the energy loss is substantial. Similar results were obtained for Ar.

As one can see in Fig. 4, Σ_{des} increases with Xe energy in both cases: when $m_{\text{eff}} = 1500$ amu, desorption occurs for Xe energies higher than about 1 eV both at normal and grazing incidence; when $m_{\text{eff}} = 150$ amu, on the contrary, the energy threshold at normal incidence (≈ 3 eV) is much larger than at grazing incidence (≈ 1 eV). In the heavy effective mass limit Σ_{des} does not depend on impact angle at large Xe energy, but it does so at low E_{Xe} . On diminishing m_{eff} , however, Σ_{des} is always much larger at grazing than at normal incidence. When m_{eff} is low, in case of normal incidence, 90% of the initial Xe energy is transferred to the surface. In contrast to this, at $\theta = 60^\circ$ this fraction is reduced to less than one half. Therefore more energy is available to desorb and eventually to dissociate, the O₂ molecule. This suggests that surface corrugation may play an essential role as it converts part of the parallel momentum of the O₂ into normal momentum allowing the molecule to go into the gas phase.

Within our simple model, it is indeed possible to simulate the corrugation c_{Ag} of the interaction potential by simply changing the radius of the Ag atom, while keeping the lattice parameter fixed: as c_{Ag} decreases the surface becomes flatter and flatter. As is apparent from Fig. 5, for a chemisorbed molecule where mirror collisions are negligible due to the low chemisorption distance, Σ_{des} may increase substantially with θ_{Xe} , decrease and even exhibit a non-monotonic behaviour, depending on the relative value of c_{Ag} , m_{eff} and E_{Xe} . For a flat surface ($c_{\text{Ag}} = 0.01 \text{ \AA}$) with negligible energy loss to the substrate ($m_{\text{eff}} = 1500 \text{ amu}$, i.e. much larger than the mass of the substrate atom), conservation of parallel momentum requires Σ_{des} to decrease with θ (\diamond in Fig. 5). When the surface–molecule interaction potential is highly corrugated ($c_{\text{Ag}} = 1.44 \text{ \AA}$) and energy loss to the substrate is substantial ($m_{\text{eff}} = 150 \text{ amu}$, i.e. comparable with the mass of the substrate atom) a large increase of Σ_{des} with θ is observed (\square in Fig. 5). In the intermediate case of a moderately corrugated potential with important energy loss to the substrate an intermediate behaviour may be observed, giving a non-monotonic angle dependence of the cross section (\times in Fig. 5). The first case resembles the low

energy behaviour of the cross section for desorption of a physisorbed system where corrugation and energy loss to phonons are negligible, like the $\text{CH}_4\text{--Ni}$ system of Beckerle et al. [5]; the second case is similar to the present $\text{O}_2\text{--Ag}(001)$ system, characterized by a substantial corrugation, as expected for a chemisorbed system and a relatively soft substrate (Ag has a lower Debye temperature than Ni and energy loss to the substrate is expected to play an important role). The intermediate case resembles the non monotonic behaviour of Σ_{des} with θ reported for the chemisorbed system $\text{NH}_3\text{--Pt}(111)$ [8], where corrugation is still significant, due to chemisorption, but not as important as for our system, the (111) surface being less corrugated than a (001) surface.

Note that the angular dependence of Σ_{des} is also strongly *energy dependent*: at large enough energy, as long as mirror collisions are negligible, the cross section is angle independent even on a strongly corrugated surface. Both the energy threshold and the energy beyond which the cross section becomes angle independent are determined by the value of m_{eff} : the higher m_{eff} the lower the energy loss to the surface and the lower the energy threshold, as apparent from Fig. 4.

These simulations not only unambiguously demonstrate that *both* corrugation *and* substantial energy loss to the substrate are required to describe the $\text{O}_2\text{--Ag}(001)$ system, but also that depending on the values of m_{eff} and corrugation a variety of different angular dependences of Σ_{des} can be obtained, as indeed experimentally observed.

A detailed inspection of the trajectories leading to desorption confirms what we anticipated before: mirror collisions (Xe surface reflections followed by Xe molecule collisions) play no role for $\text{Xe--O}_2\text{--Ag}(001)$, unlike for the $\text{Ar--CH}_4\text{--Ni}(111)$ system [5] because of the short chemisorption distance of O_2 which is partially shielded by the surrounding Ag atoms.

In conclusion we have demonstrated that energy loss to the phonon system and corrugation are the key factors in determining the angular and energetic dependence of the cross section for the desorption of O_2 , chemisorbed on a soft metal surface, and the value of the energy threshold. The large enhancement of Σ_{des} at grazing angles was not observed for previously studied systems, all of which dealt with

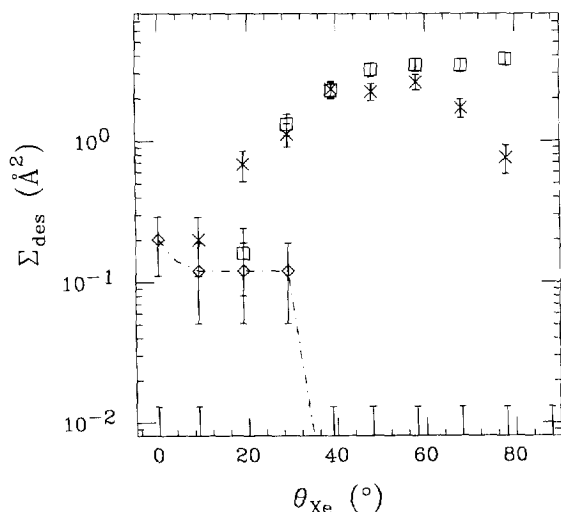


Fig. 5. Calculated cross section for desorption, as a function of θ_{Xe} for: (a) $c_{\text{Ag}} = 1.44 \text{ \AA}$, $m_{\text{eff}} = 150 \text{ amu}$ (\square); (b) $c_{\text{Ag}} = 0.36 \text{ \AA}$, $m_{\text{eff}} = 150 \text{ amu}$ (\times) and (c) $c_{\text{Ag}} = 0.01 \text{ \AA}$, $m_{\text{eff}} = 1500 \text{ amu}$ (\diamond). In cases (a) and (b) $E_{\text{Xe}} = 2 \text{ eV}$ while in case (c) $E_{\text{Xe}} = 1.4 \text{ eV}$. The dash dotted line is a guide for the eye.

harder substrates and/or with less corrugated surfaces.

Acknowledgements

We would like to thank B. Kasemo and I. Zorić for valuable discussions and for bringing our attention to the topic of collision induced processes.

References

- [1] R.R. Hudgins, P.L. Silveston, *Catal. Rev. Sci. Eng.* 11 (1975) 167.
- [2] J. Seth, R. Padiyath, S. Babu, M. David, *Thin Solid Films* 212 (1992) 251.
- [3] C. Åkerlund, I. Zorić, B. Kasemo, *J. Chem. Phys.* 104 (1996) 7359.
- [4] S.T. Ceyer, *Science* 249 (1990) 133.
- [5] J.D. Beckerle, A.D. Johnson, S.T. Ceyer, *J. Chem. Phys.* 93 (1990) 4047.
- [6] J.D. Beckerle, A.D. Johnson, Q.Y. Yang, S.T. Ceyer, *J. Chem. Phys.* 91 (1989) 5756.
- [7] D. Kulginov, M. Persson, C.T. Rettner, *J. Chem. Phys.* 106 (1997) 3370.
- [8] G. Szulczewski, R.T. Lewis, *J. Chem. Phys.* 103 (1995) 10238.
- [9] L. Romm, T. Livneh, M. Asscher, *J. Chem. Soc. Faraday Trans. 91* (1995) 3655.
- [10] C. Åkerlund, I. Zorić, B. Kasemo, A. Cupolillo, F. Buatier de Mongeot, M. Rocca, *Chem. Phys. Lett.* 270 (1997) 257.
- [11] M. Rocca, U. Valbusa, A. Gussoni, G. Maloberti, L. Racca, *Rev. Sci. Instrum.* 62 (1991) 2172.
- [12] F. Buatier de Mongeot, M. Rocca, U. Valbusa, *Surf. Sci.* 363 (1996) 68.
- [13] F. Buatier De Mongeot, A. Cupolillo, U. Valbusa, M. Rocca, *J. Chem. Phys.* 106 (1997) 9297.
- [14] F. Buatier De Mongeot, M. Rocca, A. Cupolillo, U. Valbusa, H.J. Kreuzer, S.H. Payne, *J. Chem. Phys.* 106 (1997) 711.
- [15] E.L. Garfunkel, X. Ding, G. Dong, S. Yang, X. Hou, X. Wang, *Surf. Sci.* 164 (1985) 511.
- [16] L. Vattuone, P. Gambardella, U. Valbusa, M. Rocca, *Surf. Sci.* 377-379 (1997) 671.
- [17] L. Vattuone, P. Gambardella, U. Burghaus, F. Cemič, A. Cupolillo, U. Valbusa, M. Rocca, submitted for publication.